

Spectrally resolved linewidth enhancement factor of a semiconductor frequency comb

NIKOLA OPAČAK,^{1,4}  FLORIAN PILAT,¹ DMITRY KAZAKOV,^{1,2}  SANDRO DAL CIN,¹ GEORG RAMER,³ BERNHARD LENDL,³ FEDERICO CAPASSO,² AND BENEDIKT SCHWARZ^{1,2,*} 

¹Institute of Solid State Electronics, TU Wien, Gusshausstrasse 25-25a, 1040 Vienna, Austria

²John A. Paulson School of Engineering and Applied Sciences, Harvard University, Cambridge, Massachusetts 02138, USA

³Institute of Chemical Technologies and Analytics, TU Wien, Getreidemarkt 9/164, A 1060 Vienna, Austria

⁴e-mail: nikola.opacak@tuwien.ac.at

*Corresponding author: benedikt.schwarz@tuwien.ac.at

Received 15 April 2021; revised 23 June 2021; accepted 9 August 2021 (Doc. ID 428096); published 17 September 2021

The linewidth enhancement factor (LEF) has recently moved into the spotlight of research on frequency comb generation in semiconductor lasers. Here we present a novel modulation experiment that enables direct measurement of the spectrally resolved LEF in a laser frequency comb. By utilizing a phase-sensitive technique, we are able to extract the LEF for each individual comb mode in any laser type. We first investigate and verify this universally applicable technique using Maxwell–Bloch simulations. Following, we present the experimental demonstration on a quantum cascade laser frequency comb, confirming the predicted key role of the LEF in frequency comb dynamics.

Published by The Optical Society under the terms of the [Creative Commons Attribution 4.0 License](https://creativecommons.org/licenses/by/4.0/). Further distribution of this work must maintain attribution to the author(s) and the published article's title, journal citation, and DOI.

<https://doi.org/10.1364/OPTICA.428096>

Semiconductor lasers are compact and electrically pumped and provide substantial broadband gain. They are recently gaining vast attention due to a wide range of applications that utilize their coherence properties, such as high-precision spectroscopy [1]. Their asymmetric gain spectrum additionally sets them apart from other laser types, where the lasing transition takes place between two discrete levels. Following the Kramers–Kronig relations, an asymmetric gain shape results in a dispersion curve of the refractive index that has a non-zero value at the gain peak [2]. As a consequence, a remarkable property of semiconductor lasers is that both the refractive index and the optical gain change simultaneously with the varying carrier population [3]. This property was quantified with the linewidth enhancement factor (LEF), also called the α -factor, defined by Henry as the ratio of changes of the modal index and gain [4]. Many unique properties of semiconductor lasers can be traced back to the non-zero value of this factor at the gain peak. The LEF was first introduced in the 1980s to describe the broadening of the semiconductor laser linewidth [4,5] beyond the Schawlow–Townes limit [6]. Furthermore, the LEF determines the dynamics of semiconductor lasers, as it describes the coupling

between the amplitude and phase of the optical field [7,8]. In lasers with fast gain recovery times, the LEF was recently connected to the onset of a giant Kerr nonlinearity [9] and frequency modulated combs [10]. It was shown that the light amplitude–phase coupling, quantified by the LEF, can lead to a low-threshold multimode instability and frequency comb formation [11,12]. Appropriate values of the LEF were predicted to result in the emission of solitons in active media [13]. Precise knowledge of the LEF represents a key point in understanding many astonishing features of semiconductor lasers and subsequently controlling them.

The physical origin of the non-zero LEF at the gain peak is explained through the asymmetric gain spectrum of semiconductor lasers. In interband lasers, gain asymmetry is due to the opposite curvatures of the valence and conduction bands in k -space [7], which yield LEF values $\sim 2 - 7$ [3]. In intersubband lasers, such as quantum cascade lasers (QCLs), where the states have similar curvatures, the gain asymmetry originates from the subband non-parabolicity [14], counterrotating terms [15], and Bloch gain [9]. In QCLs, measured values of the LEF range from -0.5 to 2.5 [11,16–19].

An established technique for extracting subthreshold values of the LEF is the Hakki–Paoli method by measuring the peak gain and wavelength shift [20,21]. Above threshold values can be inferred from the measurements of the linewidth broadening compared to the Schawlow–Townes limit [4] and the phase noise [22]. Other methods are based on analysis of the locking regimes induced by optical injection from a master laser [23], or on the optical feedback and characterization of the self-mixing signal [24,25]. Harder *et al.* provided a study of a single-mode laser's response under modulation of the injection current and were able to extract the LEF value [26]. In a modified experiment, heterodyne detection of a modulated single-mode QCL signal allowed a direct measurement of the LEF [16]. All of the mentioned techniques have one substantial limitation: they do not resolve the spectral dependence of the LEF. Most methods rely on single-mode operation, which is achieved either in Fabry–Pérot lasers slightly above lasing threshold or by using distributed feedback (DFB) lasers. In DFBs, the LEF is not measured at the exact position of the gain peak, since the lasing frequency is detuned. In a semiconductor optical amplifier, the LEF was measured spectrally resolved

using a tunable single-mode laser [27]. However, measuring the LEF in an amplifier does not consider the impact of gain saturation, which has been shown to affect the LEF in an operating laser [9].

In this work, we introduce a novel measurement technique that enables the direct spectrally resolved measurement of the LEF of a semiconductor laser operating in the frequency comb regime. It extends the modulation experiment used by Harder *et al.* [26] and enables extraction of the LEF for each individual comb mode from a single measurement. Each comb mode, together with its neighboring sidebands, created by RF modulation of the laser bias current, produces two beatings. The knowledge of both the amplitude and phase of these beatings enables the extraction of the LEF for every mode across the entire comb spectrum. This is made possible by shifted-wave interference Fourier transform spectroscopy (SWIFTS) [28,29], as it allows to measure the spectrally resolved amplitudes and phases of all beatings in a single-shot measurement. We first lay down the theoretical foundations of our method. Subsequently, we compare the obtained analytic values of the LEF with those extracted from numerical simulations of a single-mode laser and a laser frequency comb. This is followed by an experimental demonstration, where the method is employed on a QCL frequency comb.

In the presence of a non-zero value of the LEF, a sinusoidal modulation of the laser bias current results in both intensity modulation (IM) and optical frequency modulation (FM) of the laser output [7,26]. The optical field $E(t)$ of a modulated single-mode laser is given by

$$E(t) = \sqrt{I_0} \sqrt{1 + m \cos(2\pi f_{\text{mod}} t + \phi)} \times \cos(2\pi f t + \beta \sin(2\pi f_{\text{mod}} t + \phi + \theta)), \quad (1)$$

where I_0 is the average intensity, f is the lasing frequency, f_{mod} is the modulation frequency, and $m = \Delta I / I_0$ and $\beta = \Delta f / f_{\text{mod}}$ are the IM and FM indices, respectively, where ΔI and Δf are the amplitudes of the modulation-induced variations of the intensity

and optical frequency [30]. We include an additional arbitrary phase shift ϕ with respect to the current modulation and an FM-IM phase shift θ . The modulation of the instantaneous optical frequency is given by $f_i = f + \beta f_{\text{mod}} \cos(2\pi f_{\text{mod}} t + \phi + \theta)$.

Using the Jacobi–Anger expansion [31], we write Eq. (1) as a Fourier series (Supplement 1):

$$E(t) = \sqrt{I_0} \sum_{n=-\infty}^{+\infty} E_n \exp(2i\pi(f + n f_{\text{mod}})t). \quad (2)$$

Under the assumption of weak modulation strength ($m, \beta \ll 1$), the complex beating signals B_{\pm} between the central mode E_0 and its first modulation sidebands E_{\pm} can be written as

$$B_+ = E_+ E_0^* = e^{i(\phi+\theta)} \left(\frac{\beta}{2} + \frac{m}{4} e^{-i\theta} \right),$$

$$B_- = E_0 E_-^* = e^{i(\phi+\theta)} \left(-\frac{\beta}{2} + \frac{m}{4} e^{-i\theta} \right). \quad (3)$$

The extraction of the modulation indices m and β is possible from Eq. (3) only if both the amplitudes and phases of B_{\pm} are known. Furthermore, this is also valid in the case of a multimode laser, where each mode k produces beatings $B_{k,\pm}$ with its neighboring modulation sidebands. With knowledge of the modulation indices, the spectral LEF for each mode k can be calculated directly [3,16,18,26], and the determination of its sign is explained in Supplement 1:

$$\text{LEF}_k = 2 \frac{\beta_k}{m_k} = \frac{|B_{k,+} - B_{k,-}|}{|B_{k,+} + B_{k,-}|}. \quad (4)$$

The emission spectrum of a modulated single-mode laser is sketched in Fig. 1(a) (top) in the cases when only IM or FM is present. The corresponding beating signals B_{\pm} between the central mode and the sidebands are plotted below in the complex plane. They are in-phase with each other in the case of a pure IM, and

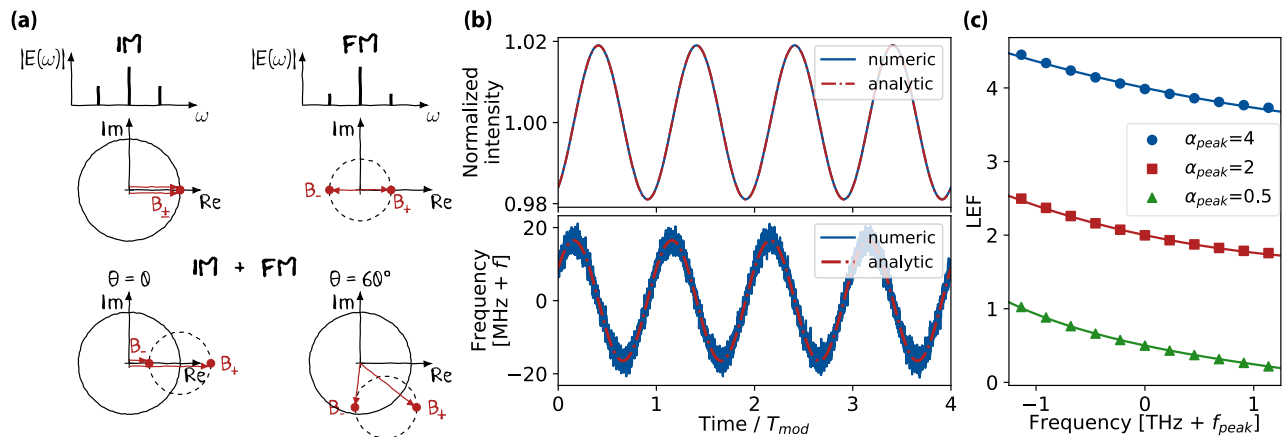


Fig. 1. Intensity modulation (IM) and frequency modulation (FM) of a single-mode laser and the LEF extraction. (a) Modulation sidebands and their beating signals B_{\pm} with the center mode in the case of a pure IM or FM (top). The beatings are represented in the complex plane (red). A mixture of both IM and FM is analyzed for two values of the IM-FM phase shift θ . (b) Simulated time traces of the laser intensity and instantaneous frequency. Analytical curves given by Eq. (1) (red dashed-dotted lines) are fitted to the numeric time traces (blue solid lines), obtained from simulation [10]. The frequency is modulated around the lasing frequency f , and the time is normalized to the modulation period T_{mod} , with $f_{\text{mod}} = 3\text{GHz}$. The phase shift between the frequency and intensity modulations is $\theta \approx \pi/2$. (c) Dependence of the calculated LEF on the lasing frequency of a simulated single-mode laser. Simulations are conducted for three values of the LEF at the gain peak α_{peak} . The lasing frequency is swept in discrete steps around the gain peak frequency f_{peak} . The values extracted by using Eq. (4) are represented with symbols. The analytic model of the LEF, given by Eq. (S14) in Supplement 1, is plotted with solid lines. The two methods are in agreement.

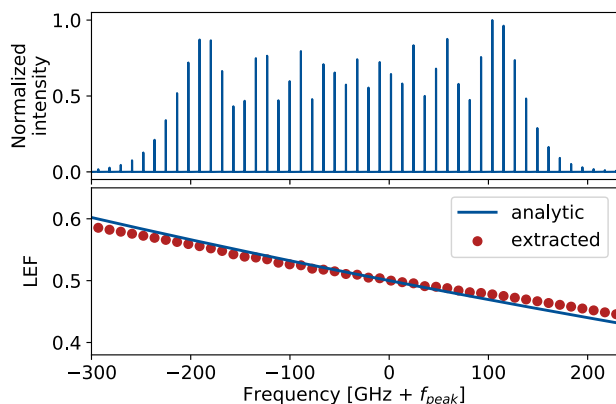


Fig. 2. LEF of a simulated multimode semiconductor laser frequency comb. The normalized intensity spectrum is depicted on the top. The spectrally resolved LEF is shown on the bottom. Red dots represent the LEF for each lasing mode, calculated using Eq. (4). The solid blue line depicts the LEF from the analytical model [Eq. (S14) in Supplement 1].

anti-phase (π phase-shifted) for a pure FM. In a modulated semiconductor laser, a mixture of IM and FM is always present, due to the coupling between the gain and the refractive index. The beating signals in this case are sketched in Fig. 1(a) for two exemplary values of the FM-IM phase shift $\theta = 0$ and $\pi/3$, which in a real experimental setting is unknown *a priori*.

In Fig. 1(b), we show the instantaneous intensity and frequency of a simulated semiconductor single-mode laser biased above threshold with a small superimposed sinusoidal modulation. We obtain them from a numerical spatiotemporal model of the laser based on the Maxwell–Bloch formalism [10,11], which additionally includes the LEF. The analytical model given by Eq. (1) is fitted to the numerical time traces of both the instantaneous intensity and frequency. The IM-FM phase shift θ approaches $\pi/2$ [Fig. 1(b)]. However, its value cannot be *a priori* assumed without measurement, since effects such as thermal and adiabatic chirp can have a large impact [18,32]. Therefore, our measurement technique removes this uncertainty by not depending on the value of θ (Eq. (4)). In Fig. 1(c), we show the extracted LEF of a simulated single-mode laser, whose lasing frequency was tuned in discrete

steps around the gain peak frequency f_{peak} . We extracted the LEF using Eq. (4). The simulations are conducted for three different values of the LEF at gain peaks $\alpha_{\text{peak}} = 0.5, 2$ and 4 , represented by green triangles, red squares, and blue circles, respectively. The extracted LEF values from the numerical model are in excellent agreement with the LEF obtained from the analytical model (solid lines) of the optical susceptibility [33,34] [Eqs. (S12) and (S14) in Supplement 1].

Now, we extend this technique to a laser frequency comb. The modulation of the laser current induces modulation sidebands around each comb mode. By finding the beatings $B_{k,\pm}$ of each mode with its sidebands, we can obtain the LEF of each comb mode. Figure 2 shows an intensity spectrum of a simulated laser in a multimode comb regime. The extracted spectrally resolved LEF is plotted with red dots below, together with the LEF from an analytical model of the laser gain medium [Eq. (S14) in Supplement 1], represented with the blue solid line. We attribute the slight deviations to coherent mechanisms that couple the frequency comb modes.

Experimentally, the amplitudes and phases of the beatings $B_{k,\pm}$ can be measured most elegantly using SWIFTS [Fig. 3(a)]. SWIFTS employs a Fourier-transform infrared (FTIR) spectrometer to spectrally resolve all individual beatings. We measure the modulation of the laser output waveform using a fast photodetector and a lock-in amplifier to obtain the SWIFTS interferogram (Fig. 1 in Supplement 1). The beatings are then obtained using the Fourier transformation. A detailed derivation of the SWIFTS spectrum can be found in Supplement 1. We extended our existing SWIFTS setup [35] with a custom-built high-resolution FTIR spectrometer (~ 500 MHz) to resolve the narrowly spaced beatings. The setup consists of a Newport Optical Delay Line Kit (using DL325), a broadband mid-infrared beam splitter, a temperature stabilized He–Ne laser, and a Zurich Instruments HF2LI lock-in amplifier for acquisition of the intensity and SWIFTS interferograms of the measured laser, as well as the interferogram of the He–Ne laser. A more detailed explanation of the experiment can be found in Supplement 1.

The QCL that we used in this measurement is a 3.5 mm long ridge laser emitting at around $8 \mu\text{m}$ and optimized for RF injection [36]. The laser was operated in a free-running frequency comb

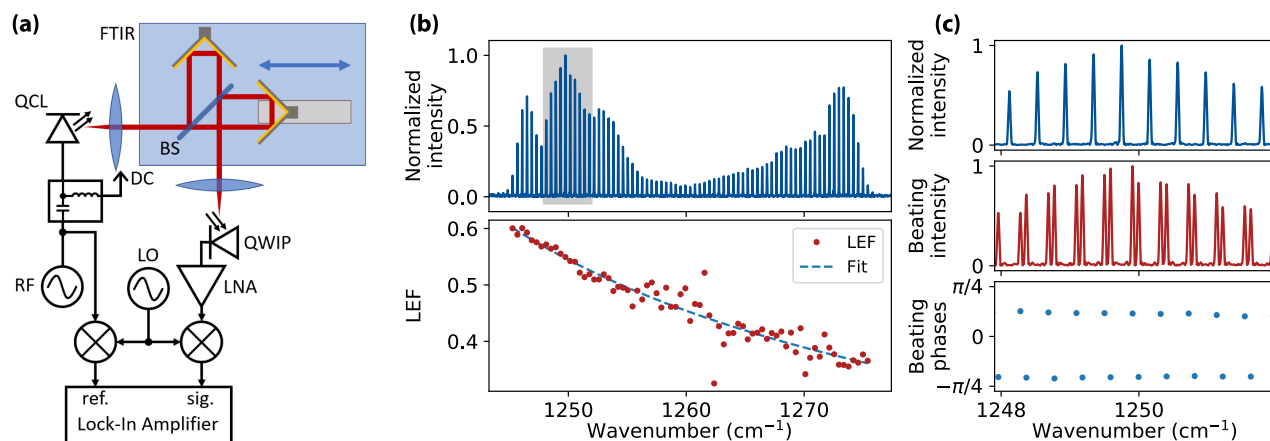


Fig. 3. Experimental data of a SWIFTS measurement with LEF evaluation. (a) Sketch of the experimental setup. FTIR, Fourier transform infrared spectrometer; BS, beam splitter; QCL, quantum cascade laser; DC, bias voltage; RF, RF generator; LO, local oscillator; QWIP, quantum well infrared photodetector; LNA, low-noise amplifier. (b) Measured intensity spectrum of the QCL and extracted LEF values for each mode (red dots) with a fit using Eq. (S14) in Supplement 1 (blue dashed line). (c) Intensity (top), beating intensity (middle), and beating phase spectrum as obtained from the SWIFTS measurement for the highlighted gray area in (b).

state with a repetition frequency of 12.2 GHz. The frequency of the weak modulation was chosen to be sufficiently lower at 9.593 GHz, and a demodulation frequency of 9.570 GHz was set on the local oscillator. For light detection, we used an RF-optimized quantum well infrared photodetector (QWIP) cooled to 78 K. The intensity spectrum [Fig. 3(b)] shows a frequency comb spanning over 75 modes. A zoom of the gray-shaded area is shown in Fig. 3(c). Although the weak modulation sidebands are not visible in the intensity spectrum (top), the amplitudes and phases of the beatings (middle and bottom, respectively) can be obtained with a high signal-to-noise ratio by using SWIFTS [Fig. 3(c)]. Using Eq. (4), we extract the LEF for each individual comb mode [Fig. 3(b), bottom]. The spectrally resolved LEF follows the expected shape [see Figs. 1(c) and 2]. Using Eq. (S14) to fit the extracted LEF, we can also infer the laser gain width above threshold. The extracted spectral LEF values match the prediction from a recent theoretical work [9], which pinpointed its origin in QCLs to the Bloch gain. The measured LEF furthermore supports its predicted key role in frequency modulated combs [10,37], as well as in ring QCLs emitting localized structures akin to dissipative Kerr solitons [11–13].

In conclusion, we present a novel technique to directly measure the spectrally resolved LEF of a running semiconductor laser frequency comb. The measurement concept is first verified using elaborate numerical simulations of a modulated semiconductor laser. There, an excellent agreement is observed with the expected spectral LEF from the analytical model. The experimental demonstration was performed on a QCL frequency comb, while the technique itself is universal. It will allow to extract the spectral LEF in frequency combs based on any type of a semiconductor laser. The LEF governs many coherent processes in a running semiconductor laser, including frequency comb operation. Its precise knowledge will provide a better fundamental understanding of light evolution, which will promote further technological advancements.

Funding. European Union's Horizon 2020 research and innovation programme (871529); Austrian Science Fund (P28914); European Research Council (853014).

Disclosures. The authors declare no conflicts of interest.

Data availability. Data underlying the results presented in this paper are not publicly available at this time but may be obtained from the authors upon reasonable request.

Supplemental document. See Supplement 1 for supporting content.

REFERENCES

1. T. W. Hänsch, *Rev. Mod. Phys.* **78**, 1297 (2006).
2. A. Yariv, *Quantum Electronics*, 3rd ed. (Wiley, 1989).
3. M. Osinski and J. Buus, *IEEE J. Quantum Electron.* **23**, 9 (1987).
4. C. Henry, *IEEE J. Quantum Electron.* **18**, 259 (1982).
5. K. Vahala and A. Yariv, *IEEE J. Quantum Electron.* **19**, 1096 (1983).
6. A. L. Schawlow and C. H. Townes, *Phys. Rev.* **112**, 1940 (1958).
7. G. P. Agrawal and N. K. Dutta, *Semiconductor Lasers* (Springer, 1995).
8. G. Gray and S. Agrawal, *IEEE Photon. Technol. Lett.* **4**, 1216 (1992).
9. N. Opačak, S. Dal Cin, J. Hillbrand, and B. Schwarz, *Phys. Rev. Lett.* **127**, 093902 (2021).
10. N. Opačak and B. Schwarz, *Phys. Rev. Lett.* **123**, 243902 (2019).
11. M. Piccardo, B. Schwarz, D. Kazakov, M. Beiser, N. Opačak, Y. Wang, S. Jha, J. Hillbrand, M. Tamagnone, W. T. Chen, A. Y. Zhu, L. L. Colombo, A. Belyanin, and F. Capasso, *Nature* **582**, 360 (2020).
12. B. Meng, M. Singleton, M. Shahmohammadi, F. Kapsalidis, R. Wang, M. Beck, and J. Faist, *Optica* **7**, 162 (2020).
13. L. Colombo, M. Piccardo, F. Prati, L. Lugiato, M. Brambilla, A. Gatti, C. Silvestri, M. Gioannini, N. Opačak, B. Schwarz, and F. Capasso, *Phys. Rev. Lett.* **126**, 173903 (2021).
14. T. Liu, K. E. Lee, and Q. J. Wang, *Opt. Express* **21**, 27804 (2013).
15. M. F. Pereira, *Appl. Phys. Lett.* **109**, 222102 (2016).
16. T. Aellen, R. Maulini, R. Terazzi, N. Hoyler, M. Giovannini, J. Faist, S. Blaser, and L. Hvozďara, *Appl. Phys. Lett.* **89**, 091121 (2006).
17. L. Jumpertz, F. Michel, R. Pawlus, W. Elsässer, K. Schires, M. Carras, and F. Grillot, *AIP Adv.* **6**, 015212 (2016).
18. A. Hangauer and G. Wysocki, *IEEE J. Sel. Top. Quantum Electron.* **21**, 74 (2015).
19. J. von Staden, T. Gensty, W. Elsässer, G. Giuliani, and C. Mann, *Opt. Lett.* **31**, 2574 (2006).
20. B. W. Hakki and T. L. Paoli, *J. Appl. Phys.* **46**, 1299 (1975).
21. I. Henning and J. Collins, *Electron. Lett.* **19**, 927 (1983).
22. C. Henry, *IEEE J. Quantum Electron.* **19**, 1391 (1983).
23. G. Liu, X. Jin, and S. Chuang, *IEEE Photon. Technol. Lett.* **13**, 430 (2001).
24. Y. Yu, G. Giuliani, and S. Donati, *IEEE Photon. Technol. Lett.* **16**, 990 (2004).
25. Y. Fan, Y. Yu, J. Xi, G. Rajan, Q. Guo, and J. Tong, *Appl. Opt.* **54**, 10295 (2015).
26. C. Harder, K. Vahala, and A. Yariv, *Appl. Phys. Lett.* **42**, 328 (1983).
27. N. Storkfelt, B. Mikkelsen, D. Olesen, M. Yamaguchi, and K. Stubkjaer, *IEEE Photon. Technol. Lett.* **3**, 632 (1991).
28. D. Burghoff, T.-Y. Kao, N. Han, C. W. I. Chan, X. Cai, Y. Yang, D. J. Hayton, J.-R. Gao, J. L. Reno, and Q. Hu, *Nat. Photonics* **8**, 462 (2014).
29. D. Burghoff, Y. Yang, D. J. Hayton, J.-R. Gao, J. L. Reno, and Q. Hu, *Opt. Express* **23**, 1190 (2015).
30. X. Zhu and D. T. Cassidy, *J. Opt. Soc. Am. B* **14**, 1945 (1997).
31. M. Abramowitz and I. A. Stegun, *Handbook of Mathematical Functions: With Formulas, Graphs, and Mathematical Tables* (Courier, 1965).
32. A. Hangauer, G. Spinner, M. Nikodem, and G. Wysocki, *Opt. Express* **22**, 23439 (2014).
33. F. Prati and L. Colombo, *Phys. Rev. A* **75**, 053811 (2007).
34. L. L. Colombo, S. Barbieri, C. Sirtori, and M. Brambilla, *Opt. Express* **26**, 2829 (2018).
35. J. Hillbrand, A. M. Andrews, H. Detz, G. Strasser, and B. Schwarz, *Nat. Photonics* **13**, 101 (2018).
36. M. R. St-Jean, M. I. Amanti, A. Bernard, A. Calvar, A. Bismuto, E. Gini, M. Beck, J. Faist, H. C. Liu, and C. Sirtori, *Laser Photon. Rev.* **8**, 443 (2014).
37. M. Dong, N. M. Mangan, J. N. Kutz, S. T. Cundiff, and H. G. Winful, *IEEE J. Quantum Electron.* **53**, 1 (2017).